**Stem Cell Reports, Volume *16***

## Supplemental Information

# Sequential regulation of hemogenic fate and hematopoietic stem and progenitor cell formation from arterial endothelium by Ezh1/2

**Rebecca A. Soto, Mohamad Ali T. Najia, Mariam Hachimi, Jenna M. Frame, Gabriel A. Yette, Edroaldo Lummertz da Rocha, Kryn Stankunas, George Q. Daley, and Trista E. North**

# Figure S1 related to Figure 1.

**A.**

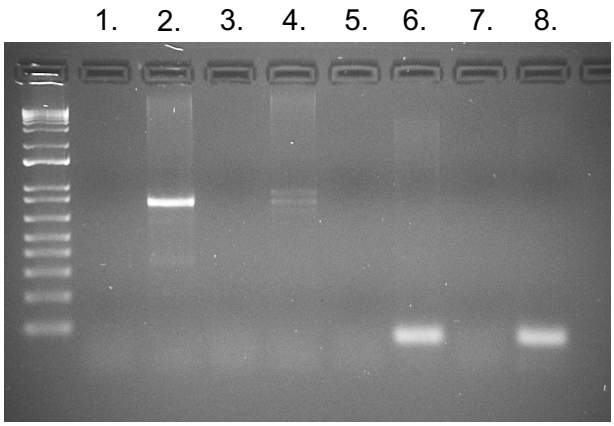


**PCR gel key:**

1. control -RT
2. control +RT
3. *ezh1* MO -RT
4. *ezh1* MO +RT
5. control -RT
6. control +RT
7. *ezh1* MO -RT
8. *ezh1* MO +RT

*ezh1* *beta-actin*

**B.**

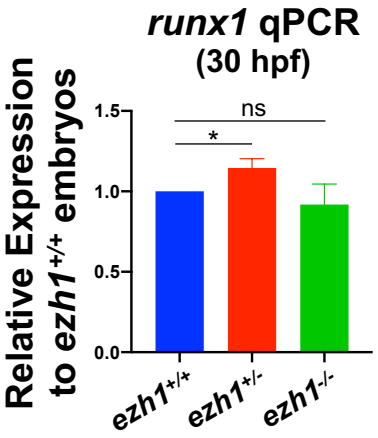

**Figure S1. *ezh1* loss increases HSPC formation, related to Figure 1**

(A) Assessment of *ezh1* splice blocking MO efficacy by PCR on cDNA prepared from 30 hpf control and *ezh1* morphant RNA. Reference gene: *b-actin*.

(B) Whole-embryo *runx1* qPCR on $ezh1^{+/+}$, $ezh1^{+/-}$, and $ezh1^{-/-}$ embryos at 30 hpf relative to 18s, normalized to average dCT of $ezh1^{+/+}$ replicate clutches ($n \geq 25$ embryos/sample x 3 replicate clutches; two-tailed unpaired Student's t test, $^{*}p < 0.05$. Mean $\pm$ SEM).

# Figure S2 related to Figure 2.

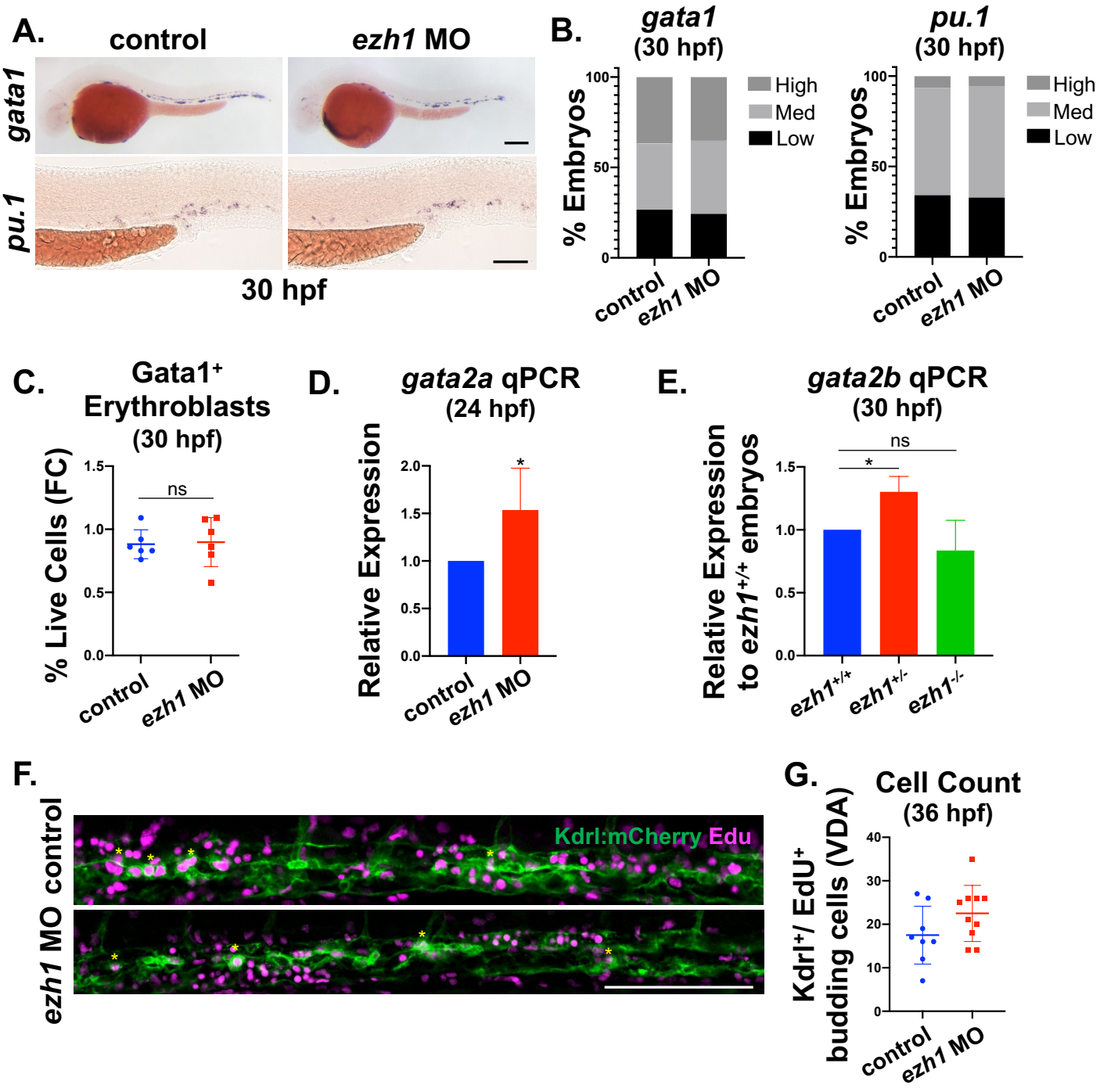

**Figure S2. Primitive erythroid and myeloid cells appear phenotypically normal in *ezh1* morphants, related to Figure 2**

(A) WISH for *gata1* (upper panels; Scale bar, 200 μm) and *pu.1* (lower panels; Scale bar, 100 μm) at 30 hpf in control and *ezh1* morphants.

(B) Qualitative phenotypic distribution plot of *gata1* embryos in (A) (n = 30 control, 37 *ezh1* morphants), and *pu.1* embryos in (A) (n = 47 control, 55 *ezh1* morphants).

(C) Flow cytometry (FC) for Gata1:dsRed$^{+}$ Erythroblasts gated on % live cells at 30 hpf in control and *ezh1* morphants (n = 5 embryos/sample x 6 biological replicates; two-tailed unpaired Student's t test, ns, not significant. Error bars indicate SD).

(D) Whole-embryo *gata2a* qPCR on control and *ezh1* morphants at 24 hpf relative to 18s ($n \geq 25$ embryos/sample x 6 replicate clutches; two-tailed unpaired Student's t test, $^{*}p < 0.05$. Mean $\pm$ SEM).

(E) Whole-embryo *gata2b* qPCR on *ezh1*$^{+/+}$, *ezh1*$^{+/-}$, and *ezh1*$^{-/-}$ embryos at 30 hpf relative to 18s, normalized to average dCT of *ezh1*$^{+/+}$ replicate clutches ($n \geq 25$ embryos/sample x 3 replicate clutches; two-tailed unpaired Student's t test, $^{*}p < 0.05$. Mean $\pm$ SEM).

(F) Confocal imaging of EdU$^{+}$ nuclei (magenta) in Kdrl:mCherry$^{+}$ embryos (green) at 36 hpf in control and *ezh1* morphants along the DA. Scale bar, 100 μm.

(G) Quantification of Kdrl$^{+}$/EdU$^{+}$ cells in (F) (n = 8 control, 10 *ezh1* morphants; two-tailed unpaired Student's t test, ns, not significant. Error bars indicate SD).

# Figure S3 related to Figure 3.

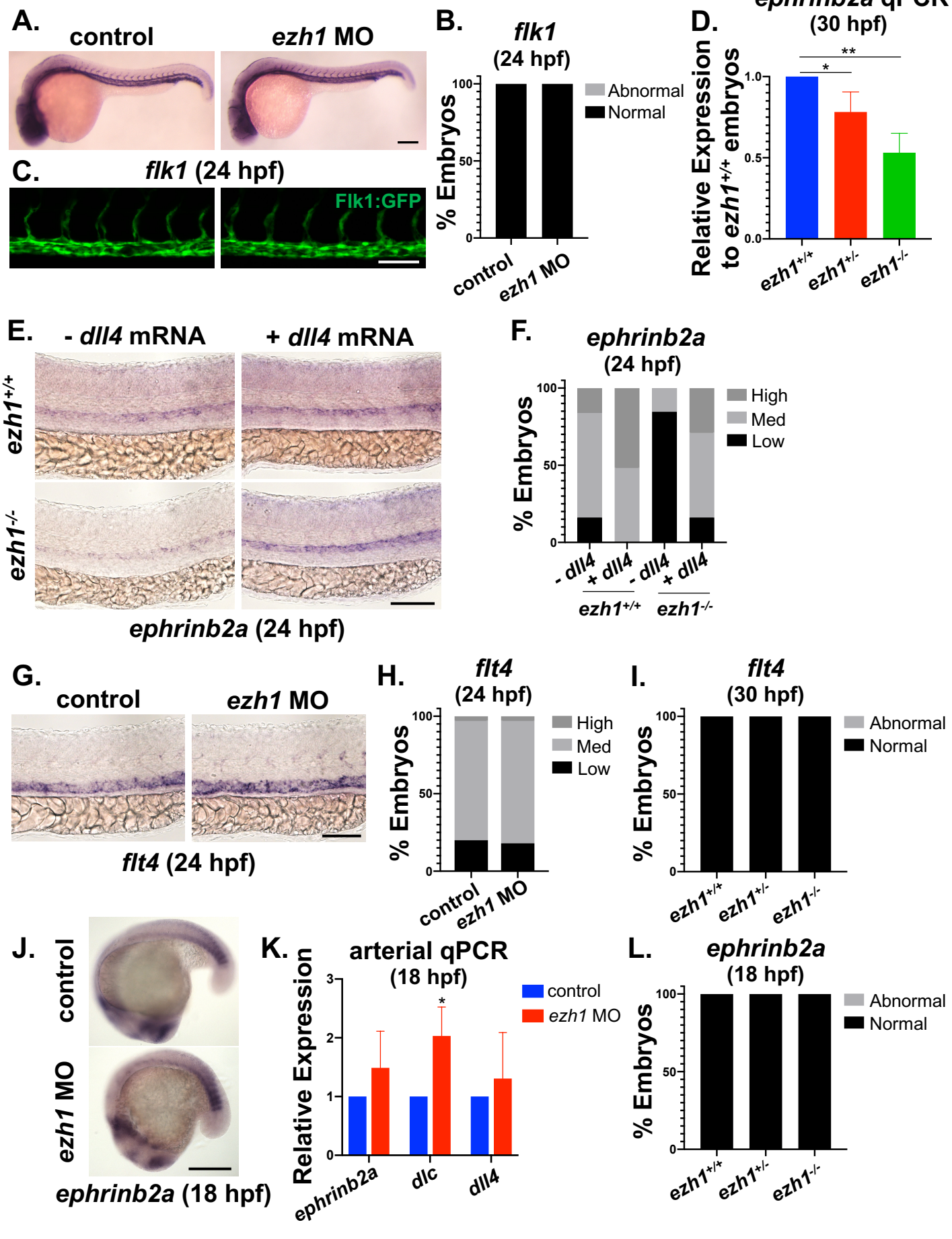

**Figure S3. Arterio-venous specification develops normally in *ezh1* morphants and mutants, related to Figure 3**

(A) WISH for *flk1* at 24 hpf in control and *ezh1* morphants. Scale bar, 200 μm.

(B) Qualitative phenotypic distribution plot of embryos in (A) (n = 33 control, 34 *ezh1* morphants).

(C) Confocal imaging on Flk1:GFP$^{+}$ control and *ezh1* morphant embryos at 24 hpf along the DA. Scale bar, 100 μm.

(D) Whole-embryo *ephrinb2a* qPCR on *ezh1*$^{+/+}$, *ezh1*$^{+/-}$, and *ezh1*$^{-/-}$ embryos at 30 hpf relative to 18s, normalized to average dCT of *ezh1*$^{+/+}$ biological replicates ($n \geq 25$ embryos/sample x 3 replicate clutches; two-tailed unpaired Student's t test, *$p < 0.05$, **$p < 0.01$. Mean ± SEM).

(E) WISH for *ephrinb2a* at 24 hpf in *ezh1*$^{+/+}$ and *ezh1*$^{-/-}$ embryos ± *dll4* mRNA injection. Scale bar, 100 μm.

(F) Qualitative phenotypic distribution plot of embryos in (E) ($n \geq 31$ embryos/condition).

(G) WISH for *flt4* at 24 hpf in control and *ezh1* morphants. Scale bar, 100 μm.

(H) Qualitative phenotypic distribution plot of embryos in (G) (n = 42 control, 41 *ezh1* morphants).

(I) Qualitative phenotypic distribution plot of WISH for *flt4* at 30 hpf on *ezh1*$^{+/+}$, *ezh1*$^{+/-}$, and *ezh1*$^{-/-}$ embryos ($n \geq 20$ embryos/genotype).

(J) WISH for *ephrinb2a* at 18 hpf in control and *ezh1* morphants. Scale bar, 250 μm.

(K) Whole-embryo qPCR for arterial markers *ephrinb2a, dlc* and *dll4* on control and *ezh1* morphants at 18 hpf relative to 18s ($n \geq 25$ embryos/sample x 3 replicate clutches; two-tailed unpaired Student's t test, *$p < 0.05$. Mean ± SEM).

(L) Qualitative phenotypic distribution plot of WISH for *ephrinb2a* at 18 hpf on *ezh1*$^{+/+}$, *ezh1*$^{+/-}$, and *ezh1*$^{-/-}$ embryos ($n \geq 35$ embryos/genotype).

# Figure S4 related to Figure 4.

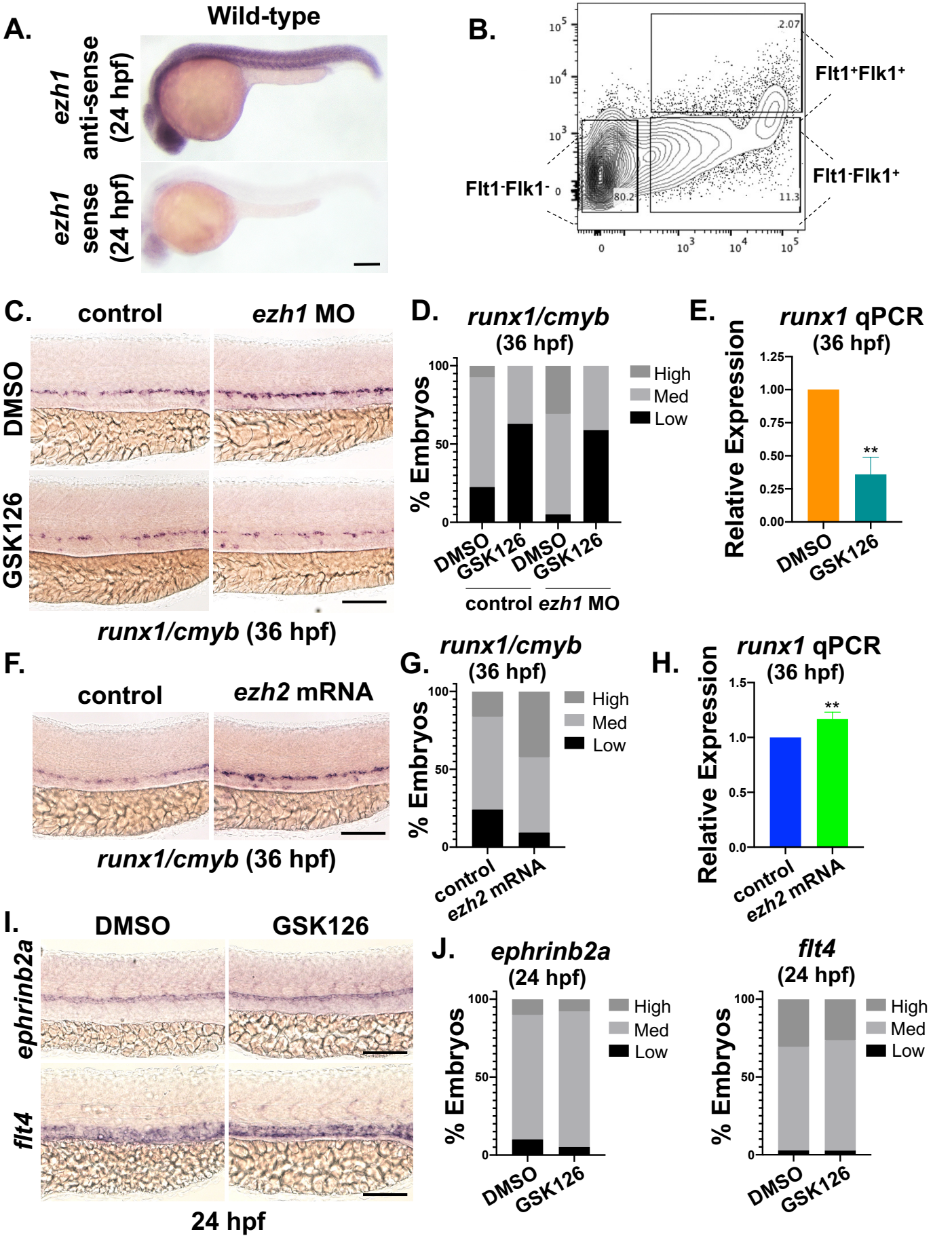

**Figure S4. Differential *ezh* requirements for endothelial maintenance and HSPC formation, related to Figure 4**

(A) WISH using an *ezh1* anti-sense probe (upper panel) and *ezh1* sense probe (lower panel) at 24 hpf in wild-type embryos. Scale bar, 200 μm.

(B) FACS plot for cell sorting at 30 hpf using Flk1:GFP and Flt1:tdTomato reporter lines.

(C) WISH for *runx1/cmyb* at 36 hpf in control and *ezh1* morphants ± DMSO/1 μM GSK126 treatment from 12-36 hpf. Scale bar, 100 μm.

(D) Qualitative phenotypic distribution plot of embryos in (C) ($n \geq 34$ embryos/condition).

(E) Whole-embryo *runx1* qPCR on DMSO and 1 μM GSK126 treated embryos from 12-36 hpf relative to 18s ($n \geq 25$ embryos/sample x 3 replicate clutches; two-tailed unpaired Student's t test, $^{**}p < 0.01$. Mean ± SEM).

(F) WISH for *runx1/cmyb* at 36 hpf in control and *ezh2* mRNA injected embryos. Scale bar, 100 μm.

(G) Qualitative phenotypic distribution plot of embryos in (F) (n = 62 control, 64 *ezh2* mRNA injected embryos).

(H) Whole-embryo *runx1* qPCR on control and *ezh2* mRNA injected embryos at 36 hpf relative to 18s ($n \geq 25$ embryos/sample x 3 replicate clutches; two-tailed unpaired Student's t test, $^{**}p < 0.01$. Mean ± SEM).

(I) WISH for *ephrinb2a* (upper panels) and *flt4* (lower panels) at 24 hpf on DMSO and 1 μM GSK126 treated embryos from 12-24 hpf. Scale bars, 100 μm.

(J) Qualitative phenotypic distribution plot of *ephrinb2a* embryos in (I) (n = 40 DMSO, 39 1 μM GSK126 treated embryos), and *flt4* embryos in (I) (n = 36 DMSO, 38 1 μM GSK126 treated embryos).

# Figure S5 related to Figure 5.

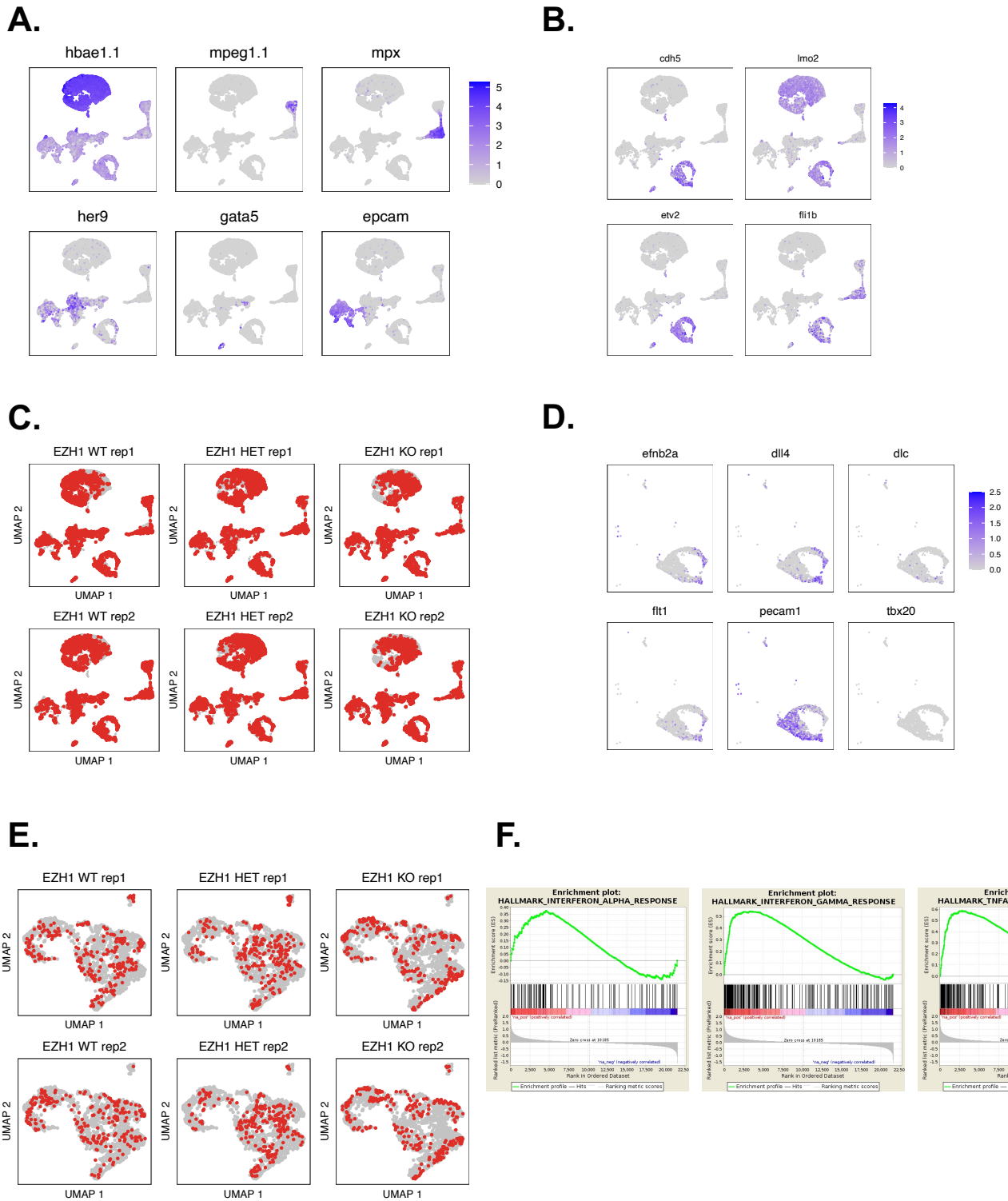

**Figure S5. scRNA-seq of *ezh1* mutant embryos reveals biological differences, related to Figure 5**
(A) UMAP plot showing *hbae1.1, mpeg1.1, mpx, her9, gata5,* and *epcam* expression to verify cluster identity designations.
(B) UMAP plot showing *cdh5, lmo2, etv2* and *fli1b* expression each localize to the endothelial cell clusters.
(C) UMAP plot visualizing each technical replicate across *ezh1* genotypes.
(D) UMAP plot showing arterial *efnb2a, dll4, dlc, flt1,* and *tbx20* as well as *pecam1* expression localize to the endothelial cell clusters.
(E) UMAP plot visualizing each technical replicate across *ezh1* genotypes after re-clustering on the EC populations.
(F) GSEA of day 28 $CD34^{+}CD38^{-}$ HSPCs 5F plus shEZH1 compared to 5F plus shLUC cells from Vo et al., 2018 (n = 10 shEZH1, 8 shLUC samples).

# Figure S6 related to Figure 6.

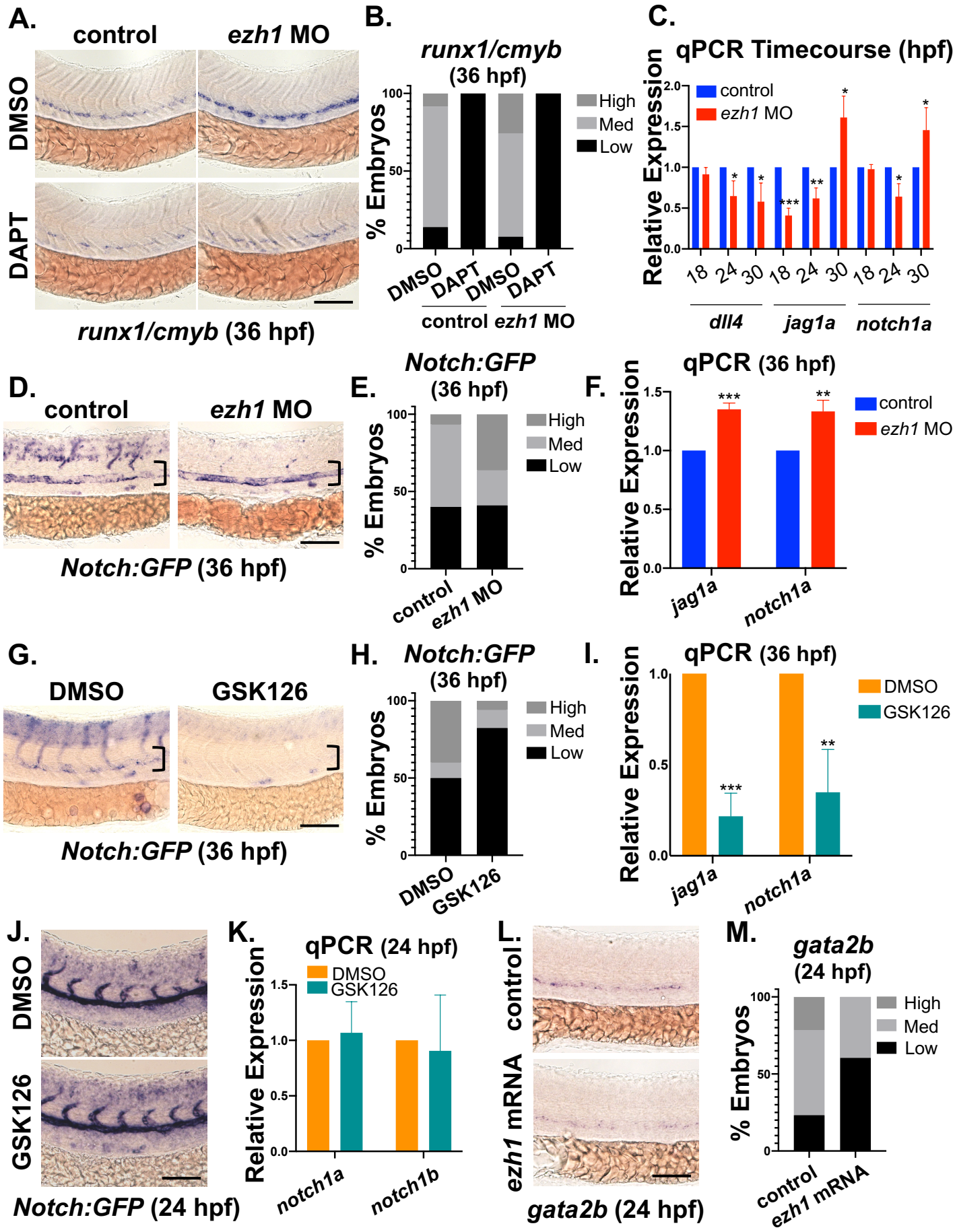

**Figure S6. HSPC expansion mediated by Notch activity is specific to Ezh1 knockdown, related to Figure 6**

(A) WISH for *runx1/cmyb* at 36 hpf in control and *ezh1* morphants ± DMSO/100 μM DAPT treatment from 12-36 hpf. Scale bar, 100 μm.

(B) Qualitative phenotypic distribution plot of embryos in (A) ($n \geq 34$ embryos/condition).

(C) Whole-embryo *dll4, jag1a* and *notch1a* qPCR on control and *ezh1* morphants at 18, 24 and 30 hpf relative to 18s ($n \geq 25$ embryos/sample x 3 replicate clutches/timepoint; two-tailed unpaired Student's t test, $^{*}p < 0.05$, $^{**}p < 0.01$, $^{***}p < 0.001$. Mean ± SEM).

(D) WISH for *GFP* on Notch:GFP$^{+}$ control and *ezh1* morphant embryos at 36 hpf along the DA. Scale bar, 100 μm.

(E) Qualitative phenotypic distribution plot of embryos in (D) ($n \geq 48$ embryos/condition).

(F) Whole-embryo *jag1a* and *notch1a* qPCR on control and *ezh1* morphants at 36 hpf relative to 18s ($n \geq 25$ embryos/sample x 3 replicate clutches; two-tailed unpaired Student's t test, $^{**}p < 0.01$, $^{***}p < 0.001$. Mean ± SEM).

(G) WISH for *GFP* in the DA on Notch:GFP$^{+}$ DMSO and 1 μM GSK126 treated (12-36 hpf) embryos. Scale bar, 100 μm.

(H) Qualitative phenotypic distribution plot of embryos in (G) ($n \geq 20$ embryos/condition).

(I) Whole-embryo *jag1a* and *notch1a* qPCR on DMSO and 1 μM GSK126 treated (12-26 hpf) embryos relative to 18s ($n \geq 25$ embryos/sample x 3 replicate clutches; two-tailed unpaired Student's t test, $^{**}p < 0.01$, $^{***}p < 0.001$. Mean ± SEM).

(J) WISH for *GFP* in the DA on Notch:GFP$^{+}$ DMSO and 1 μM GSK126 treated (12-24 hpf) embryos. Scale bar, 100 μm.

(K) Whole-embryo *notch1a* and *notch1b* qPCR on DMSO and 1 μM GSK126 treated (12-24 hpf) embryos relative to 18s ($n \geq 25$ embryos/sample x 3 replicate clutches; two-tailed unpaired Student's t test, ns, not significant. Mean ± SEM).

(L) WISH for *gata2b* at 24 hpf in control and *ezh1* mRNA injected embryos. Scale bar, 100 μm.

(M) Qualitative phenotypic distribution plot of embryos in (L) (n = 56 control, 53 *ezh1* mRNA injected embryos).

**SUPPLEMENTAL EXPERIMENTAL PROCEDURES**

**Zebrafish Transgenic/Mutant lines and Mouse Mutant line** (related to Experimental Model and Subject Details)

| **Zebrafish: Official Name** | **Common Name** | **Reference** |
|---|---|---|
| *Tg(-6.0itga2b:EGFP)*$^{la2}$ | CD41:eGFP | (Bertrand et al., 2008) |
| *Tg(kdrl:Has.HRAS-mCherry)*$^{s916}$ | Kdrl:mCherry | (Hogan et al., 2009) |
| *Tg(gata1a:dsRed)* | Gata1:dsRed | (Traver et al., 2003) |
| *Tg(lmo2:EGFP)* | Lmo2:eGFP | (Zhu et al., 2005) |
| *Tg(EPV:Tp1-MmuHbb:EGFP)* | Notch:GFP | (Parsons et al., 2009) |
| *Tg(-0.8flt1:tdTomato)* | Flt1:tdTomato | (Bussmann et al., 2010) |
| *Tg(kdrl:GFP)*$^{la116}$ | Flk1:GFP | (Choi et al., 2007) |
| *Tg(rag2:GFP)* | Rag2:GFP | (Langenau et al., 2003) |
| *Tg(-6tal1:EGFP)* | Scl:GFP | (Zhang and Rodaway, 2007) |
| *Tg(hsp70l:1xMYC-notch1a-intra)*$^{fb12}$ | Hsp70:NICD | (Zhao et al., 2014) |
| *ezh1*$^{b1394/b1394}$ | *ezh1*$^{-/-}$ | (Yette et al., 2021) |
| *Tg(cmyb:EGFP)*$^{zf169}$ | cMyb:GFP | (North et al., 2007) |
| *TgBAC(gata2b:KalTA4)*$^{sd32}$*; Tg(UAS:lifeact-GFP)*$^{mu271}$ | Gata2b:Gal4; UAS:lifeactGFP | (Butko et al., 2015); (Helker et al., 2013) |
| *ezh1*$^{b1394/b1394}$*; Tg(kdrl:EGFP)*$^{s843}$ | *ezh1*$^{-/-}$; Flk1:eGFP | (Yette et al., 2021); (Jin et al., 2005) |
| **Mouse: Official Name** | **Common Name** | **Reference** |
| *Ezh1*$^{tm1Jnw/tm1Jnw}$ | *Ezh1*$^{-/-}$ | (Ezhkova et al., 2011) |

**Morpholino Sequence**

| **Name** | **Sequence** | **ZFN ID** | **Reference** |
|---|---|---|---|
| MO1-*ezh1* | 5’ TGTGATTTCTACACACCTCTCCACA 3’ | ZDB-MRPHLNO-141118-18 | (Huang et al., 2013) |

**Chemical Modulators**

| **Chemical** | **Source** | **Identifier** |
|---|---|---|
| GSK126 | Selleck Chemicals | S7061 |
| DAPT | Selleck Chemicals | S2215 |

**SUPPLEMENTAL EXPERIMENTAL PROCEDURES**

**Oligos**

| **D. rerio Gene** | **Forward primer** | **Reverse primer** | **Reference** |
|---|---|---|---|
| ***gata2b* (qPCR)** | ACCACCACACTCTGGAGAC | CTGTTGCGTGTCTGAATACC | Butko et al., 2015 |
| ***gata2a* (qPCR)** | TCTTGAATCACTTGGACTCG | GGACTGTGTATGAGGTGTGG | Butko et al., 2015 |
| ***runx1* (qPCR)** | CGTCTTCACAAACCCTCCTCAA | GCTTTACTGCTTCATCCGGCT | Carroll et al., 2014 |
| ***ephrinb2a* (qPCR)** | CAAGGACAGCAAATCGAATG | TGAGCCAATGACTGATGAGG | Carroll et al., 2014 |
| ***dll4* (qPCR)** | TGGCCAGTTATCCTGTCTCC | CTCACTGCATCCCTCCAGAC | Carroll et al., 2014 |
| ***dlc* (qPCR)** | CGCAGAAACCTCTGACCAGT | CAGTCCTCACTGATAGCGAGTC | Carroll et al., 2014 |
| ***tbx20* (qPCR)** | AGATTGACAGCAACCCGTTT | TGCTGAATGTCCTTCTTCTCC | Carroll et al., 2014 |
| ***ezh1* (qPCR)** | AGGAAGCGTCTAGTGAGGTCT | ACGGCGATTTGACTGGAACA | San et al., 2016 |
| ***ezh2* (qPCR)** | ACTTTGAGCTCCTCCACACG | CAACCAGTGCGGCAATTTCA | Zhong et al., 2018 |
| ***notch1a* (qPCR)** | CATCTACTGCGACGTGCCTA | CCTGCATCAACACACTGACC | Gerri et al., 2018 |
| ***jag1a* (qPCR)** | ATTGGTGGATACTTCTGCGAGT | CCATTCACCAGATCCTTACACA | Monteiro et al., 2016 |
| ***18s* (qPCR)** | TCGCTAGTTGGCATCGTTTAT | CGGAGGTTCGAAGACGATCA | Carroll et al., 2014 |
| ***b-actin*** | TCTGTCCCATGCCAACCAT | TGCCCTCGTGCTGTTTT | Lim et al., 2017 |
| ***ezh1* (sense probe)** | TAATACGACTCACTATAGGGA AAAGAGAAACATGCTTACGGG CGACTGA | CTGCACATGCAGGCTTCTAAT | This study |
| ***ezh1* (antisense probe)** | CATGCTTACGGGCGACTGA | TAATACGACTCACTATAGGGA AAAGAGAAACTGCACATGCA GGCTTCTAAT | This study |
| ***dll4* (mRNA generation)** | ATTTAGGTGACACTATAGCATCG GTGCGCTCACTGTGGAA | CGGCCGCGACCTGCAGCTCGAGC AC (Amplifying/Sequencing) | This study |

| **D. rerio Gene** | **Forward primer** | **Reverse primer** | **Reference** |
|---|---|---|---|
| ***notch1b* (qPCR)** | GTCTCAGCCCTGCCAGAAC | GCATTTAGGCTCATGGGTGA | Gerri et al., 2018 |
| ***ezh2 (sorted cell qPCR)*** | AAATCGGAGAAGGGTCCTGT | TCTGTTGGAGCTGAACATGC | San et al., 2016 |
| ***ezh2* (mRNA generation)** | ATTTAGGTGACACTATAGATTCTGAGTATAAACGACAGAC | CGGCCGCGACCTGCAGCTCGAGCAC (Amplifying/Sequencing) | This study |
| ***ezh1* (mutant genotyping)** | GGCTGAATGTTTGTGGCTTTTTCACC | GGAAGTTGAACCGTGGCACCTG | (Yette et al., 2021) |

**SUPPLEMENTAL EXPERIMENTAL PROCEDURES**
**Antibodies/Kits/Constructs/Reagents**

| Name | Source | Identifier |
|---|---|---|
| CD117 APC-eFluor780 | eBioscience | 47-1171-82 |
| CD41a PE-Cy7 | eBioscience | 25-0411-82 |
| CD16/32 PE | eBioscience | 12-0161-82 |
| Ter119 APC | BD | 557909 |
| Zebrafish Ephrin-B2 Antibody | R&D Systems | AF1088 |
| Donkey anti-Goat IgG (H+L) Secondary Antibody, Alexa Fluor 647 | Invitrogen | A-21447 |
| DAPI | Sigma Aldrich | D9542 |
| Click-iT™ EdU Cell Proliferation Kit for Imaging, Alexa Fluor™ 647 dye | Invitrogen | C10340 |
| mMessage mMachine™ SP6 Transcription Kit | Invitrogen | AM1340 |
| RNAqueous Total RNA Isolation Kit | Invitrogen | AM1912 |
| TURBO DNA-free Kit | Invitrogen | AM1907 |
| SuperScript III First-Strand Synthesis SuperMix for qRT-PCR | Invitrogen | 11752050 |
| SuperScript VILO cDNA Synthesis Kit | Invitrogen | 11-754-050 |
| RNeasy Micro Kit | Qiagen | 74004 |
| SYBR Green PCR Master Mix | Applied Biosystems | 44-729-18 |
| Liberase TM | Sigma | 5401127001 |
| Type I collagenase | Sigma | C0130 |
| SYTOX Red dead cell stain | Thermo Fisher Scientific | S34859 |
| pExpress-1 *ezh1* plasmid | Horizon Discovery | MDR1734-202779115 |
| pME18S-FL3 *dll4* plasmid | Horizon Discovery | MDR1734-202795513 |
| pME18S-FL3 *ezh2* plasmid | Horizon Discovery | MDR1734-202729457 |

## SUPPLEMENTAL EXPERIMENTAL PROCEDURES

### *ezh1* morpholino validation

Splicing efficiency of MO1-*ezh1* was determined by PCR on 30 hpf control and *ezh1* morphant cDNA using the following primers: *ezh1*ExonFW: 5' TCTCGATGTCCCAGTCCCAT 3' and *ezh1*ExonRV: 5' TCCCTTTTCGAGTGGCATCC 3'. We used *b-actin* qPCR primers as an internal reference gene, sequences listed in oligos table. Results were analyzed on a 2% agarose gel in Figure S1A.

### Zebrafish Immunohistochemistry

Wild-type and *ezh1* morphants were fixed in 4% paraformaldehyde at room temperature for 2 hours, washed with 1X PBS/0.1%Tween, and stored at 4°C prior to immunohistochemistry. Embryos were blocked/permeabilized with PBS-3% BSA containing 1% Tx100 and incubated with the following antibodies: Zebrafish Ephrin-B2 pAB (1:100 primary, R&D Systems), Alexa Fluor 647 secondary antibody (Invitrogen) was used for immunofluorescence and DAPI (10 μg/mL, Sigma Aldrich). N = 3 biological replicates, representative images are shown.

### EdU Proliferation Assay

EdU labeling was used to assess cell proliferation; Kdrl:mCherry$^{+}$ embryos were incubated at 4°C with 500 μM EdU/10% DMSO in E3 water for 1 hour, fixed in 4% paraformaldehyde, permeabilized with 1% Triton for 1 hour, and labeled using the Click-iT EdU Proliferation Kit (Molecular Probes, Invitrogen) for 1 hour at room temperature in accordance to the manufacturer's protocol.

### Single-cell RNA-Sequencing

Single-cell RNA-seq was performed on the 10X Genomics Chromium platform using single cell expression 3' v2 profiling chemistry. Following Flk:GFP$^{+}$ FACS, cells from each *ezh1* genotype were loaded across two lanes in a 10X Genomics Single Cell 3' Chip as independent technical replicates and libraries were constructed according to the manufacturer's protocol. Cells were loaded into 10X lanes at cell concentrations to maintain an estimated doublet rate below 5%. The final libraries were assayed via an Agilent High Sensitivity dsDNA Bioanalyzer, normalized, pooled and shallow sequenced (Illumina MiniSeq), identifying ~11,000 high confidence cell barcodes in total across all libraries. The libraries were renormalized per the distribution of reads/library from the shallow sequencing run and deep sequenced on a NovaSeq S4 (Illumina) to a depth of ~100,000 reads per cell with cycle configuration 151-8-8-151.

### Single-cell RNA-Sequencing Analysis

A custom *Danio rerio* reference genome containing a GFP transcript was generated using Ensembl Release 101 (ftp://ftp.ensembl.org/pub/release-101/gtf/danio_rerio/) with the mkref command from cellranger v2.1 (10X Genomics). Sequencing data was aligned to the custom reference and subsequently processed with cellranger count. Raw count matrices for each library were read into R and analyzed with Seurat v3.2. High-quality cells were retained based on technical metrics: <5% mitochondrial reads, >1000 UMI counts, and >500 genes detected. Count matrix normalization, scaling and variable feature selection was performed with an SCT transform with regression of the proportion of mitochondrial reads. Principle component analysis was performed and the first 15 PCs were utilized for clustering after visual inspection of the proportion of variance explained by each PC. Graph-based clustering was performed with FindClusters() and visualized via a UMAP embedding. Differentially enriched genes were identified for each cluster with FindMarkers() and clusters annotated according to literature-supported marker genes. Cells defined as endothelium were subset from the raw count matrix and re-clustered with 20 PCs per an analogous procedure used for the full dataset. Differentially expressed genes were identified between genotypes or clusters as log2(fold-change) < -0.25 or log2(fold-change) > 0.25 and a Benjamini-Hochberg -corrected FDR < 0.05. Gene ontogeny analysis was performed using GOrilla (Eden et al., 2009).

## SUPPLEMENTAL EXPERIMENTAL PROCEDURES

### quantitative PCR data analysis

Data analysis used the delta/delta Ct method with fold-change calculated to controls for each biological clutch for whole-embryo qPCR. Relative expression level in *ezh1* mutants was calculated by averaging the dCt of *ezh1*$^{+/+}$ biological clutches and using the delta/delta Ct method with fold-change of each biological replicate within *ezh1*$^{+/-}$ and *ezh1*$^{-/-}$ genotypes against average dCt of stage-matched *ezh1*$^{+/+}$ embryos. qPCR for FACS-isolated samples calculated relative to 18s.

**SUPPLEMENTAL REFERENCES**


Bertrand, J.Y., Kim, A.D., Teng, S., and Traver, D. (2008). CD41$^{+}$ cmyb$^{+}$ precursors colonize the zebrafish pronephros by a novel migration route to initiate adult hematopoiesis. Development *135*, 1853-1862.

Bussmann, J., Bos, F.L., Urasaki, A., Kawakami, K., Duckers, H.J., and Schulte-Merker, S. (2010). Arteries provide essential guidance cues for lymphatic endothelial cells in the zebrafish trunk. Development *137*, 2653-2657.

Butko, E., Distel, M., Pouget, C., Weijts, B., Kobayashi, I., Ng, K., Mosimann, C., Poulain, F.E., McPherson, A., Ni, C.W., Stachura, D.L., Del Cid, N., Espín-Palazón, R., Lawson, N.D., Dorsky, R., Clements, W.K., and Traver, D. (2015). Gata2b is a restricted early regulator of hemogenic endothelium in the zebrafish embryo. Development *142*, 1050-1061.

Carroll, K.J., Esain, V., Garnaas, M.K., Cortes, M., Dovey, M.C., Nissim, S., Frechette, G.M., Liu, S.Y., Kwan, W., Cutting, C.C., Harris, J.M., Gorelick, D.A., Halpern, M.E., Lawson, N.D., Goessling, W., and North, T.E. (2014). Estrogen Defines the Dorsal Ventral Limit of VEGF Regulation to Specify the Location of the Hemogenic Endothelial Niche. Dev. Cell *29*, 437-453.

Choi, J., Dong, L., Ahn, J., Dao, D., Hammerschmidt, M., and Chen, J.-N. (2007). FoxH1 negatively modulates *flk1* gene expression and vascular formation in zebrafish. Dev. Biol. *304*, 735-744.

Eden, E., Navon, R., Steinfeld, I., Lipson, D., and Yakhini, Z. (2009). GOrilla: a tool for discovery and visualization of enriched GO terms in ranked gene lists. BMC Bioinformatics *10,* 48

Ezhkova, E., Lien, W.-H., Stokes, N., Pasolli, H.A., Silva, J.M., and Fuchs, E. (2011). EZH1 and EZH2 cogovern histone H3K27 trimethylation and are essential for hair follicle homeostasis and wound repair. Genes Dev. *25*, 485-498.

Gerri, C., Marass, M., Rossi, A., and Stainer, D.Y.R. (2018). Hif-1$\alpha$ and Hif-2$\alpha$ regulate hemogenic endothelium and hematopoietic stem cell formation in zebrafish. Blood *131*, 963-973.

Helker, C.S.M., Schuermann, A., Karpanen, T., Zeuschner, D., Belting, H.-G., Affolter, M., Schulte-Merker, S., and Herzog, W. (2013). The zebrafish common cardinal veins develop by a novel mechanism: lumen ensheathment. Development *140*, 2776-2786.

Hogan, B.M., Bos, F.L., Bussmann, J., Witte, M., Chi, N.C., Duckers, H.J., and Schulte-Merker, S. (2009). Ccbe1 is required for embryonic lymphangiogenesis and venous sprouting. Nat. Genet. *41*, 396-398.

Huang, H.T., Kathrein, K.L., Barton, A., Gitlin, Z., Huang, Y.H., Ward, T.P., Hofmann, O., Dibiase, A., Song, A., Tyekucheva, S., Hide, W., Zhou, Y., and Zon, L.I. (2013). A network of epigenetic regulators guides developmental haematopoiesis in vivo. Nat. Cell Biol. *15*, 1516-1525.

Jin, S.-W., Beis, D., Mitchell, T., Chen, J.-N., and Stainer, D.Y.R. (2005). Cellular and molecular analyses of vascular tube and lumen formation in zebrafish. Development *132*, 5199-5209.

Langenau, D.M., Traver, D., Ferrando, A.A., Kutok, J.L., Aster, J.C., Kanki, J.P., Lin, S., Prochownik, E., Trede, N.S., Zon, L.I., and Look, A.T. (2003). Myc-Induced T cell Leukemia in Transgenic Zebrafish. Science *299*, 887-890.

Lim, S.-E., Esain, V., Kwan, W., Theodore, L.N., Cortes, M., Frost, I.M., Liu, S.Y., and North, T.E. (2017). HIF1$\alpha$-induced PDGFR$\beta$ signaling promotes developmental HSC production via IL-6 activation. Exp. Hematol. *46*, 83-95.

Monteiro, R., Pinheiro, P., Joseph, N., Peterkin, T., Koth, J., Repapi, E., Bonkhofer, F., Kirmizitas, A., and Patient, R. (2016). Transforming Growth Factor β Drives Hemogenic Endothelium Programming and the Transition to Hematopoietic Stem Cells. Dev. Cell *38*, 358-370.

North, T.E., Goessling, W., Walkley, C.R., Lengerke, C., Kopani, K.R., Lord, A.M., Weber, G.J., Bowman, T.V., Jang, I.H., Grosser, T., FitzGerald, G.A., Daley, G.Q., Orkin, S.H., and Zon, L.I. (2007). Prostaglandin E2 regulates vertebrate haematopoietic stem cell homeostasis. Nature *447*, 1007-1011.

Parsons, M.J., Pisharath, H., Yusuff, S., Moore, J.C., Siekmann, A.F., Lawson, N., and Leach, S.D. (2009). Notch-responsive cells initiate the secondary transition in larval zebrafish pancreas. Mech. Dev. *126*, 898-912.

San, B., Chrispijn, N.D., Wittkopp, N., van Heeringen, S.J., Lagendijk, A.K., Aben, M., Bakkers, J., Ketting, R.F., and Kamminga, L.M. (2016). Normal formation of a vertebrate body plan and loss of tissue maintenance in the absence of *ezh2*. Sci. Rep. *6*, 24658.

Traver, D., Paw, B.H., Poss, K.D., Penberthy, W.T., Lin, S., and Zon, L.I. (2003). Transplantation and *in vivo* imaging of multilineage engraftment in zebrafish bloodless mutants. Nat. Immuno. *4*, 1238-1246.

Yette, G. A., Stewart, S., and Stankunas, K. (2021). Zebrafish Polycomb repressive complex-2 critical roles are largely Ezh2- over Ezh1-driven and concentrate during early embryogenesis. BioRxiv, doi: https://doi.org/10.1101/2020.12.31.424918.

Zhang, X.Y., and Rodaway, A.R.F. (2007). SCL-GFP transgenic zebrafish: in vivo imaging of blood and endothelial development and identification of the initial site of definitive hematopoiesis. Dev. Biol. *307*, 179-194.

Zhao, L., Borikova, A.L., Ben-Yair, R., Guner-Ataman, B., MacRae, C.A., Lee, R.T., Burns, C.G., and Burns, C.E. (2014). Notch signaling regulates cardiomyocyte proliferation during zebrafish heart regeneration. PNAS *111(4)*, 1403-1408.

Zhong, Y., Ye, Q., Chen, C., Wang, M., and Wang, H. (2018). Ezh2 promotes clock function and hematopoiesis independent of histone methyltransferase activity in zebrafish. Nuc. Acids. Res. *46*, 3382-3399.

Zhu, H., Traver, D., Davidson, A.J., Dibiase, A., Thisse, C., Thisse, B., Nimer, S., and Zon, L.I. (2005). Regulation of the *lmo2* promoter during hematopoietic and vascular development in zebrafish. Dev. Biol. *281*, 256-269.